Modelling charge transport lengths in heterojunction solar cells

K. P. Musselman,[1,a)] Y. Ievskaya,[2] and J. L. MacManus-Driscoll[2]
[1]*Optoelectronics Group, Department of Physics, University of Cambridge, Cambridge CB3 0HE, United Kingdom*
[2]*Device Materials Group, Department of Materials Science and Metallurgy, University of Cambridge, Cambridge CB2 3QZ, United Kingdom*

(Received 12 July 2012; accepted 26 November 2012; published online 17 December 2012)

A drift-diffusion model is used to estimate the minority carrier transport length and depletion width in heterojunction solar cells from measured external quantum efficiency (EQE) data. The model is applied to Cu_2O-ZnO heterojunctions synthesized by electrodeposition and thermal oxidation, and the electron drift and diffusion lengths are estimated: $L_{drift} \approx 110$ nm for electrodeposited Cu_2O and $L_{drift} \approx 2790$ nm and $L_{diff} \approx 310$ nm for thermally oxidized Cu_2O. Better fitting of EQE data is obtained than with traditional models that neglect recombination in the depletion region. © *2012 American Institute of Physics*. [http://dx.doi.org/10.1063/1.4771981]

The external quantum efficiency (EQE) is the ratio of collected electrons to incident photons at a particular wavelength λ in an absorbing semiconductor. For a heterojunction solar cell, the EQE can be expressed as

$$EQE(\lambda) = \int_0^T \eta_{CE}(x) g(x,\lambda) dx / I_0(\lambda), \quad (1)$$

where η_{CE} is the minority carrier collection efficiency as a function of depth x in the absorber layer, $g(x, \lambda)$ is the charge generation rate in the absorber, $I_0(\lambda)$ is the incident photon flux, and T is the absorber thickness. The EQE of a variety of photovoltaics (PV), including Si,[1,2] CdTe,[3,4] and Cu_2O-ZnO (Refs. 5 and 6) has been modelled to provide useful information about minority carrier collection lengths, although the breadth of this work has likely been limited by the availability of accurate EQE and absorption coefficient α values for the various materials. Gärtner derived an expression for the EQE of an absorbing semiconductor, which has formed the basis of most previous work and is a function of the depletion layer width W, minority carrier diffusion length L_{diff}, α, and λ[7]

$$EQE(\lambda) = 1 - \frac{\exp(-\alpha(\lambda)W)}{1 + L_{diff}\alpha(\lambda)}. \quad (2)$$

Fig. 1(a) displays the η_{CE} for the traditional Gärtner model. An infinite absorber thickness ($T = \infty$) and complete collection from the depletion region ($\eta_{CE} = 100\%$ for $x < W$) are assumed. In the case of thin film PV, the assumption of an infinite absorber layer thickness may be inaccurate, which has led others to develop 1D transport models with appropriate boundary conditions.[5,8] However, the assumption that no recombination occurs in the depletion region (complete collection) is still inherent in these models. This assumption may not be accurate in all materials, particularly solution-processed absorbers with low mobility-lifetime products. In depleted-heterojunction colloidal quantum dot solar cells, for example, the depletion width is expected to extend through the active layer, yet internal quantum efficiencies are $< 100\%$ for most λ, suggesting significant recombination within the depletion layer.[9] Recent studies have indicated that the depletion layer thickness in electrodeposited Cu_2O-ZnO solar cells may be on the order of a micron,[10] while reported short-circuit current densities indicate an electron transport length below 1 μm.[11] This suggests that minority electrons in electrodeposited Cu_2O may be collected primarily by drift from the depletion region rather than diffusion from the bulk. Thus, it is clear that recombination within the depletion layer should be considered when modelling the charge transport of some low cost PV. Here, we determine electron transport lengths in Cu_2O-ZnO solar cells by modelling their measured EQE. The model used is general in nature; it can account for recombination within the depletion region and may therefore provide more accurate estimations of the electron transport length than reported previously for Cu_2O-ZnO PV.[5,6]

Cuprous oxide (Cu_2O) has received attention due to the relative abundance of copper, a good theoretical power conversion efficiency, and the availability of different synthesis techniques such as thermal oxidation of Cu, sputtering, pulsed laser deposition, and electrodeposition.[12,13] The operational mechanisms of Cu_2O-based PV, however, are not well established and the efficiency of these devices has remained correspondingly low. Cu_2O heterojunctions have received the most attention, with Cu_2O-ZnO devices being the most effective to date.[12] In Cu_2O-ZnO cells, electron-hole pairs are created by the absorption of light in Cu_2O. Majority holes are transported through the Cu_2O to a collection electrode, and minority electrons are transported to the Cu_2O-ZnO interface, then through the ZnO for collection, as illustrated in Fig. 1(b). It is expected that electrons created within the Cu_2O depletion region adjacent to the ZnO drift to the interface, whereas those created by absorption deeper in the Cu_2O must first diffuse to the depletion region. The distance that electrons can be transported in Cu_2O will depend on the device architecture as well as the material properties. The ability to accurately determine electron transport lengths in these devices is crucial for the design of suitable architectures. Electrodeposited Cu_2O-ZnO devices, for example,

a)Electronic mail: kpdm2@cam.ac.uk.

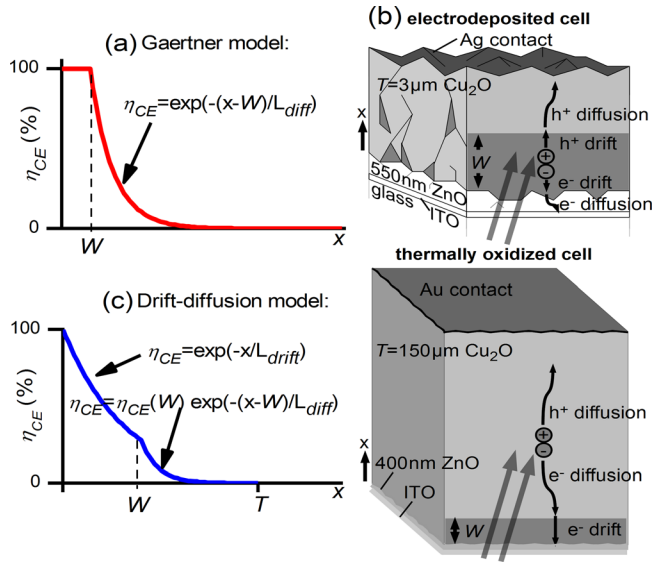

FIG. 1. (a, c) Models of minority carrier collection efficiency η_{CE} vs. depth x in the absorber layer: Gärtner model (a), drift-diffusion model used here for absorber layers of thickness T (c). (b) Schematics of solar cell architectures studied here with depletion width W and charge transport processes noted.

have been nanostructured in order to improve charge collection but have yet to demonstrate better efficiencies than bilayer architectures.[11]

Fig. 1(c) displays the model of η_{CE} employed in this work, which accounts for recombination in the depletion region. Following the work of Galluzzi, the collection probability for a minority carrier in the depletion layer can be expressed as[14]

$$\eta_{CE}(x < W) = \exp(-x/L_{drift}), \tag{3}$$

where L_{drift} is a characteristic drift length for the minority carriers in the depletion region. Assuming that minority carriers in the bulk of the absorbing layer diffuse to the boundary of the depletion region, the η_{CE} for carriers in the bulk can be taken as

$$\eta_{CE}(x > W) = \exp(-W/L_{drift})\exp(-(x-W)/L_{diff}). \tag{4}$$

If reflection, scattering, and parasitic absorption effects are neglected, the charge generation rate in the absorbing layer as a function of depth can be expressed as[15]

$$g(x,\lambda) = I_0(\lambda)\alpha(\lambda)\exp(-\alpha(\lambda)x). \tag{5}$$

Combining Eq. (5) and the η_{CE} given in Eq. (3), the minority carrier collection rate resulting from absorption in the depletion layer ($0 < x < W$) of the absorber can be expressed as

$$\int_0^W \exp\left(\frac{-x}{L_{drift}}\right) g(x,\lambda)dx = \frac{I_0(\lambda)\alpha(\lambda)}{\frac{1}{L_{drift}} + \alpha(\lambda)}\left[1 - \exp\left(-W\left(\frac{1}{L_{drift}} + \alpha(\lambda)\right)\right)\right]. \tag{6}$$

Similarly, the carrier collection rate from the bulk of the absorbing layer ($W < x < T$) is expected to be

$$\int_W^T \exp\left(\frac{-W}{L_{drift}}\right)\exp\left(\frac{-(x-W)}{L_{diff}}\right) g(x,\lambda)dx = \frac{I_0(\lambda)\alpha(\lambda)\exp\left(W\left(\frac{1}{L_{diff}} - \frac{1}{L_{drift}}\right)\right)}{\frac{1}{L_{diff}} + \alpha(\lambda)} \times \left[\exp\left(-W\left(\frac{1}{L_{diff}} + \alpha(\lambda)\right)\right) - \exp\left(-T\left(\frac{1}{L_{diff}} + \alpha(\lambda)\right)\right)\right]. \tag{7}$$

Summing Eqs. (6) and (7) gives the total minority carrier collection rate for the whole thickness T of the absorber layer modelled in Fig. 1(c). It follows that

$$EQE(\lambda) = \frac{\text{Eq. (6)} + \text{Eq. (7)}}{I_0(\lambda)}. \tag{8}$$

Equation (8) gives the EQE for a heterojunction in which recombination within the depletion layer may occur. It is similar to the expression derived by Galluzzi, with the exception that a finite absorber thickness has been considered here, rather than an infinite value.[14] However, inherent to this model is the assumption that the absorber is sufficiently thick that $T > W$ and that reflection and recombination effects at the back electrode are negligible. The model is based on an expected η_{CE} (Eqs. (3) and (4)) and is general in nature, i.e., for large T and $L_{drift} \gg W$, Eq. (8) reduces to that of Gärtner (Eq. (2)). It neglects reflection and parasitic absorption losses and it assumes efficient majority carrier transport. We find that with the inclusion of an appropriate scaling factor $(1-\varphi_{loss}(\lambda))$ in Eq. (8) to account for these losses, this generalized formula can accurately model Cu_2O-ZnO heterojunctions with varying minority carrier transport lengths (L_{drift}, L_{diff}).

Electrodeposited bilayer Cu_2O-ZnO solar cells consisting of approximately 3 μm Cu_2O and 550 nm ZnO layers on ITO/glass were synthesized as reported previously and their EQEs measured under short-circuit conditions.[10] A traditional Gärtner model (Eq. (2)) was first fit to the data with W and L_{diff} as variables. As the error in the measured EQE values is expected to scale with the magnitude of the EQE, a least-squares percentage regression was employed to ensure the fit was weighted equally across the wavelength range.[16] Published values for $\alpha(\lambda)$ of electrodeposited Cu_2O were found to vary widely and are often only presented for limited λ ranges,[17] such that more reliable values reported for sputtered Cu_2O thin films and thermally oxidized Cu_2O foils were employed (shown in the supplemental material[21]).[18] The $(1-\varphi_{loss}(\lambda))$ scaling factor was also used with the Gärtner model, and transmission data provided by the ITO/glass manufacturer (Praezisions Glas & Optik GmbH; included in the supplemental material) were used to estimate $\varphi_{loss}(\lambda)$. The fits obtained for the Gärtner model are shown as the solid lines in Fig. 2(a), and the squared residuals of the

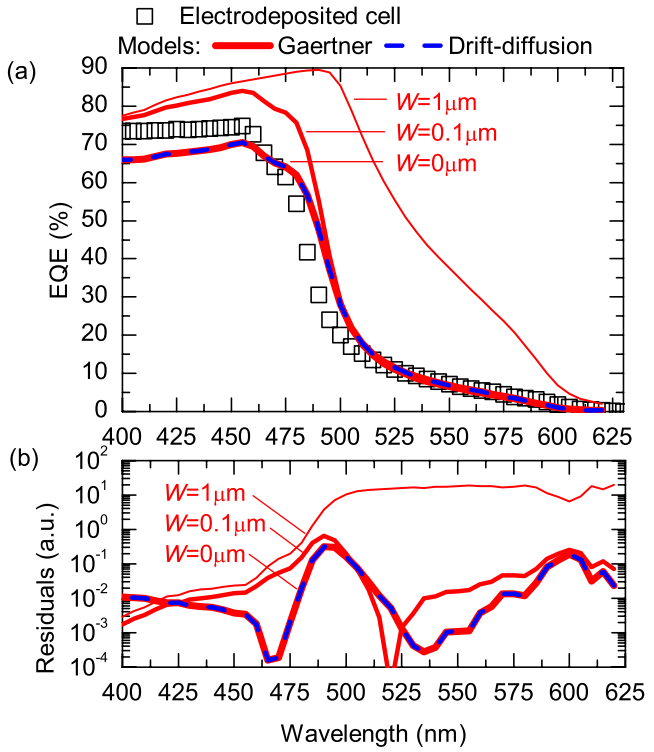

FIG. 2. (a) EQE data for an electrodeposited Cu_2O-ZnO cell and fits obtained with the Gärtner and drift-diffusion models. The best fits for the two models are similar, as $W = 0$ gave the best fit to the Gärtner model. Fits to the Gärtner model where W was held at non-zero values of 0.1 μm and 1 μm are also shown. (b) Squared residuals of the various fits.

fits are given in Fig. 2(b). The Gärtner model is found to most accurately reproduce the experimental data when $W = 0$ (fits for $W = 0.1$ μm and $W = 1$ μm are also shown for comparison). The $W = 0$ condition corresponds to the elimination of the lossless depletion region, such that a η_{CE} and fit similar to that of the Drift-diffusion model (also shown in Fig. 2) results.

The complete drift-diffusion model presented in Eq. (8) was fit to the data with L_{drift}, L_{diff}, and W as the variables. The same $\varphi_{loss}(\lambda)$ values and $T = 3$ μm were employed. The derivation of Eq. (8) necessitates that W is less than or equal to T. L_{drift} and L_{diff} can be related by[14]

$$\frac{L_{drift}}{F} = \frac{L_{diff}^2 q}{kT}, \tag{9}$$

where q, k, and T are the electron charge, Boltzmann's constant, and temperature, respectively, and F is the mean electric field of the depletion layer, which can be approximated as $F = V_{bi}/W$, where V_{bi} is the built-in bias of the heterojunction. The fitting was therefore performed with L_{drift} and L_{diff} constrained by Eq. (9), with V_{bi} limited to a value between 0.4 V and 1.1 V, the expected range for this heterojunction. A physically meaningful value of $W = 3$ μm is obtained using the drift-diffusion model (versus $W = 0$ for the Gärtner model). Fitting indicated a L_{drift} of approximately 150 nm for the electrodeposited Cu_2O (values summarized in Table I). The fact that L_{drift} is less than W for this solution emphasizes that recombination in the depletion layer is an important consideration when modelling charge transport in these devices.

It is noted that inherent in these models is the assumption that the path travelled by the light through the absorbing semiconductor is perpendicular to the film surface and interfaces. However, light incident on the rough ITO/ZnO/Cu_2O interfaces is expected to be scattered, resulting in an angular distribution of light in the Cu_2O. If an effective transmission angle of θ relative to the film normal is assumed in order to account for scattering, the carrier generation rate in the absorber (Eq. (5)) becomes

$$g(x,\lambda) = \frac{I_0(\lambda)\alpha(\lambda)}{\cos\theta(\lambda)} \exp(-\alpha(\lambda)x/\cos\theta(\lambda)). \tag{10}$$

Modified versions of the Gärtner (Eq. (2)) and drift-diffusion (Eq. (8)) models result, which include this scattering correction (listed in the supplemental material). Here, a simple wavelength-independent value of $\theta = 45°$ was considered to approximate random scattering in all directions from the rough ZnO-Cu_2O interface. The experimental data were fit with the two models and this correction. The fitted data and squared residuals are shown in the supplemental material and are almost identical to those obtained without the scattering correction in Fig. 2. The values obtained for L_{drift}, L_{diff}, and W, however, are reduced when scattering is accounted for, as can be seen in Table I. This analysis suggests that minority electrons have a drift length of approximately 108 nm in the electrodeposited device and $W = 2.7$ μm. Further modelling of light scattering in these devices and direct measurement of α for electrodeposited Cu_2O will allow more accurate values of L_{drift}, L_{diff}, and W to be obtained; however, these results strongly suggest that recombination within the depletion region should be accounted for when modelling the EQE of these devices.

Finally, to emphasize the general nature of the charge collection model presented here, Eq. (8) was used to fit EQE data of a thermally oxidized Cu_2O-ZnO heterojunction, where larger transport lengths are expected. The Cu_2O was

TABLE I. Fitted device parameters for the electrodeposited cell.

Model	L_{drift} (nm)	L_{diff} (nm)	W (μm)	Mean squared residual (a.u.)
Assuming normal light transmission				
Gärtner model (Eq. (2))	…	153	0	0.042
Drift-diffusion model (Eq. (8))	153	111	3.00	0.042
With scattering correction ($\theta = 45°$)				
Gärtner model (Eq. (2))	…	108	0	0.042
Drift-diffusion model (Eq. (8))	108	100	2.70	0.042

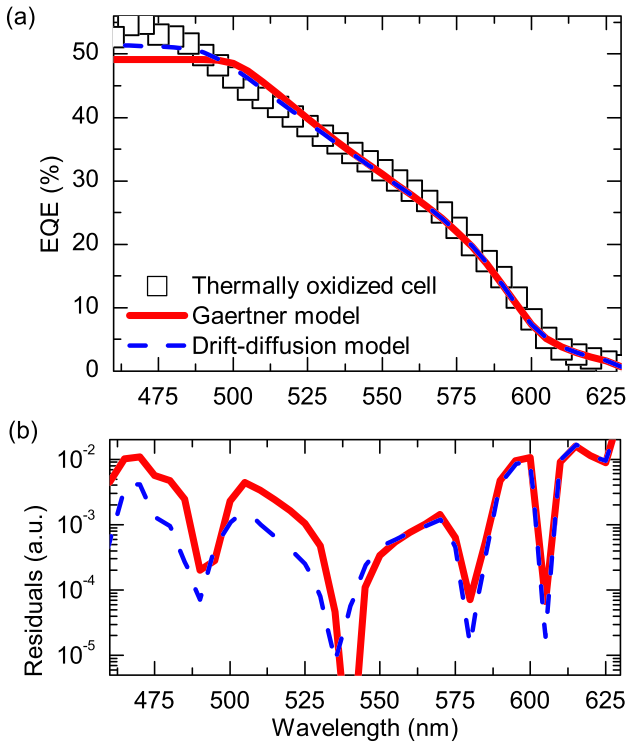

FIG. 3. (a) EQE data for a thermally oxidized Cu_2O-ZnO cell and fits obtained with the two models. (b) Squared residuals of the fits.

prepared by thermally oxidizing 100 μm Cu foils (99.999%, Alfa Aesar) at 950 °C in O_2-Ar gas with an oxygen partial pressure of 20 000 ppm for 1 h, and an approximately 400 nm ZnO layer was deposited on the Cu_2O by atmospheric chemical vapor deposition at 150 °C.[19] Au contacts were evaporated on the Cu_2O, and a semi-transparent ITO contact was sputtered on the ZnO using an Emitech sputter coater.

The experimental EQE values are presented in Fig. 3(a), along with the fits obtained using our drift-diffusion model (Eq. (8)) and that of Gärnter (Eq. (2)). Least-squares fitting was again applied to the relative errors for $\lambda > 475$ nm; a decrease in the EQE was seen at shorter wavelengths, which may be due to optical effects or other recombination processes at the ZnO-Cu_2O interface, such as majority carrier diffusion,[20] that are not accounted for in the models. The same $\alpha(\lambda)$ values were used, and as no prior information was available for $\varphi_{loss}(\lambda)$ in the thermally oxidized device, it was allowed to vary but assumed wavelength-independent. T was 150 μm, and L_{drift} and L_{diff} were again constrained by Eq. (9). Fitting was performed with and without a scattering correction ($\theta = 45°$). Fitted values for both cases are given in Table II and the scatter-corrected fits and residuals, which are similar to those in Fig. 3, are again included in the supplemental material. While both models replicate the experimental data well, smaller residuals are obtained with the drift-diffusion model. The mean squared residuals are approximately an order of magnitude smaller than for the electrodeposited cells. This may be due to the α values being more suitable here, since they were obtained from similar thermally oxidized foils. As expected, the electron transport lengths determined for the thermally oxidized Cu_2O are higher than those obtained for the electrodeposited Cu_2O ($L_{drift} = 2788$ nm cf. $L_{drift} = 108$ nm). Nonetheless, the solution to the drift-diffusion model suggests that recombination in the depletion region may still be relevant in the thermally oxidized cell, e.g., inserting values from Table II in Eq. (3) gives $\eta_{CE}(W) < 60\%$. The large φ_{loss} value of 48% indicates that almost half the potential charges may be lost to scattering, parasitic absorption, and majority carrier losses in this device.

In summary, a generalized model for the EQE of a heterojunction solar cell (Eq. (8)) has been applied to Cu_2O-ZnO devices made by electrodeposition and thermal oxidation. The drift-diffusion model allows for minority carrier recombination throughout the entire absorber layer, whether it be a thin electrodeposited layer or thick thermally oxidized foil. A number of approximations have been employed in this modelling: (i) simple estimates for reflection, scattering, and parasitic absorption have been made and efficient majority carrier transport assumed, (ii) it is assumed that the depletion region can be modelled by a mean electric field, (iii) variations in W with light intensity have been neglected, (iv) possible contributions from excitons in Cu_2O have been neglected,[6] (v) the cells were assumed to be sufficiently thick that reflection and recombination effects at the back electrode could be neglected, and (vi) errors in the wavelength have been taken as negligible. Further work can be done to characterize these parameters and additional measurements, such as determination of the V_{bi} and α, white light bias EQE, and irradiation from both sides of the cell,[5] can be performed to further characterize accuracy. Nonetheless, the drift-diffusion model was found to describe EQE data of both electrodeposited and thermally oxidized Cu_2O heterojunction solar cells better than the traditional Gärtner model and provide useful parameters for device design and optimization. Electron drift and diffusion lengths of $L_{drift} = 108$ nm (electrodeposited Cu_2O), and $L_{drift} = 2788$ nm, $L_{diff} = 313$ nm (thermally oxidized Cu_2O) were obtained, with an estimated

TABLE II. Fitted device parameters for the thermally oxidized cell.

Model	L_{drift} (nm)	L_{diff} (nm)	W (μm)	φ_{loss} (%)	Mean squared residual (a.u.)
Assuming normal light transmission					
Gärtner model (Eq. (2))	…	973	1.05	50.9	0.0049
Drift-diffusion model (Eq. (8))	3942	443	2.15	48.0	0.0042
With scattering correction ($\theta = 45°$)					
Gärtner model (Eq. (2))	…	688	0.74	50.9	0.0049
Drift-diffusion model (Eq. (8))	2788	313	1.52	48.0	0.0042

light scattering correction. In both cases, L_{drift} is on the order of the fitted depletion thickness ($W = 2.7\ \mu$m for electrodeposited and $W = 1.5\ \mu$m for thermally oxidized Cu_2O) or smaller, clearly indicating that recombination in the depletion layer warrants consideration. It is however noted that the magnitude of W and L_{drift} will depend on the properties of the materials and heterointerface, such that in some situations recombination in the depletion region may be negligible. Material and device characterization should be continued in parallel with modelling to ensure the most accurate description. Finally, while Cu_2O has been the focus of this work, the presented model can be equally applied to other heterojunctions where recombination in the depletion layer might be expected.

K.P.M. would like to thank Girton College (Cambridge), who have funded this work. Y.I. acknowledges the Cambridge Overseas Trust. J.L.M-D. acknowledges funding from the ERC NOVOX 247276 Advanced Investigator grant.

[1]C. R. Wronski, B. Abeles, and G. D. Cody, Sol. Cells **2**, 245 (1980).
[2]S. S. Hegedus, R. E. Rocheleau, W. Buchanan, and B. N. Baron, J. Appl. Phys. **61**, 381 (1987).
[3]J. Toušek, Phys. Status Solidi A **128**, 531 (1991).
[4]K. H. Herrmann, A. E. Rakhshani, and L. Alshamary, Solid-State Electron. **43**, 1251 (1999).
[5]Y. Liu, H. K. Turley, J. R. Tumbleston, E. T. Samulski, and R. Lopez, Appl. Phys. Lett. **98**, 162105 (2011).
[6]F. Biccari, C. Malerba, and A. Mittiga, Sol. Energy Mater. Sol. Cells **94**, 1947 (2010).
[7]W. W. Gärtner, Phys. Rev. **116**, 84 (1959).
[8]A. G. Milnes and D. Feucht, *Heterojunctions and Metal-Semiconductor Junctions* (Academic, New York, USA, 1972).
[9]A. G. Pattantyus-Abraham, I. J. Kramer, A. R. Barkhouse, X. Wang, G. Konstantatos, R. Debnath, L. Levina, I. Raabe, M. K. Nazeeruddin, M. Grätzel *et al.*, ACS Nano **4**, 3374 (2010); O. E. Semonin, J. M. Luther, S. Choi, H. Chen, J. Gao, A. J. Nozik, and M. C. Beard, Science **334**, 1530 (2011).
[10]K. P. Musselman, A. Marin, L. Schmidt-Mende, and J. L. MacManus-Driscoll, Adv. Funct. Mater. **22**, 2202 (2012).
[11]K. P. Musselman, A. Wisnet, D. C. Iza, H. C. Hesse, C. Scheu, J. L. MacManus-Driscoll, and L. Schmidt-Mende, Adv. Mater. **22**, E254 (2010).
[12]A. Mittiga, E. Salza, F. Sarto, M. Tucci, and R. Vasanthi, Appl. Phys. Lett. **88**, 163502 (2006); M. Izaki, T. Shinagawa, K. T. Mizuno, Y. Ida, M. Inaba, and A. Tasaka, J. Phys. D:Appl. Phys. **40**, 3326 (2007).
[13]K. Akimoto, S. Ishizuka, M. Yanagita, Y. Nawa, G. K. Paul, and T. Sakurai, Sol. Energy **80**, 715 (2006); A. Chen, H. Long, X. Li, Y. Li, G. Yang, and P. Lu, Vacuum **83**, 927 (2009).
[14]F. Galluzzi, J. Phys. D: Appl. Phys. **18**, 685 (1985).
[15]J. Nelson, *The Physics of Solar Cells* (Imperial College Press, London, UK, 2003).
[16]P. B. Sáez and B. E. Rittmann, Water Res. **26**, 789 (1992); C Tofallis, J. Mod. Appl. Stat. Methods **7**, 526 (2008).
[17]P. E. de Jongh, D. Vanmaekelbergh, and J. J. Kelly, Chem. Mater. **11**, 3512 (1999); J. Electrochem. Soc. **147**, 486 (2000); T. Mahalingam, J. Chitra, S. Rajendran, and P. Sebastian, Semicond. Sci. Technol. **17**, 565 (2002).
[18]C. Malerba, F. Biccari, C. L. A. Ricardo, M. D'Incau, P. Scardi, and A. Mittiga, Sol. Energy Mater. Sol. Cells **95**, 2848 (2011).
[19]L. Dunlop, A. Kursumovic, and J. L. MacManus-Driscoll, Appl. Phys. Lett. **93**, 172111 (2008).
[20]J. Reichman, Appl. Phys. Lett. **38**, 251 (1981).
[21]See supplemental material at http://dx.doi.org/10.1063/1.4771981 for absorption coefficient data used and scattering-corrected equations and fits to experimental data.